Glycoconj J (2009) 26:623–633
DOI 10.1007/s10719-008-9179-8

# Brain lipid composition in grey-lethal mutant mouse characterized by severe malignant osteopetrosis

**Alessandro Prinetti · Federica Rocchetta · Elvira Costantino · Annalisa Frattini · Elena Caldana · Francesca Rucci · Arianna Bettiga · Pietro L. Poliani · Vanna Chigorno · Sandro Sonnino**

Received: 5 May 2008 / Revised: 6 August 2008 / Accepted: 8 August 2008 / Published online: 10 September 2008


**Abstract** The grey-lethal mouse (*gl*/*gl*) mutant most closely resembles the severe human malignant autosomal recessive OSTM1-dependent form of osteopetrosis that it has been described to be associated with neurological abnormalities. For this reason, we have analyzed the brain lipid composition (gangliosides, neutral glycosphingolipids, phospholipids and cholesterol), from *gl*/*gl* mice at different ages of development and compared with wild type mice. Both cholesterol and glycerophospholipid content and pattern in the *gl*/*gl* and control mice were very similar. In contrast, significant differences were observed in the content of several sphingolipids. Higher amount of the monosialogangliosides GM2 and GM3, and lower content of sphingomyelin, sulfatide and galactosylceramide were observed in the *gl*/*gl* brain with respect to controls. The low content of sphingomyelin, sulfatide and galactosylceramide is consistent with the immunohistochemical results showing that in the grey-lethal brain significant depletion and disorganization of the myelinated fibres is present, thus supporting the hypothesis that loss of function of the OSTM1 causes neuronal impairment and myelin deficit.

**Keywords** Sphingolipids · Gangliosides · Myelin · Demyelination · Ostepetrosis

**Abbreviations**

| | |
|---|---|
| *gl*/*gl* | grey-lethal |
| ARO | Autosomal Recessive Osteopetrosis |
| OSTM1 | osteopetrosis associated transmembrane protein 1 |
| HSC | haematopoietic stem cells |
| HPTLC | high-performance thin layer chromatography |

## Introduction

Infantile malignant Autosomal Recessive Osteopetroses (ARO-MIM 259700, 259720, 611497, 259710) are severe hereditary bone diseases characterized by increased bone density due to a defect in osteoclastic bone resorption or differentiation [1].

The generalized bone sclerosis causes, in ARO patients, a number of severe clinical manifestations, including: macrocephaly, cranial nerve dysfunction such as deafness and blindness, hepatosplenomegaly, anemia and pancytopenia due to severe bone marrow failure beginning in fetal life or in early infancy. The prognosis has a fatal outcome, generally within the first decade of life.

A. Prinetti · F. Rocchetta · V. Chigorno · S. Sonnino
Center of Excellence on Neurodegenerative Diseases,
Department of Medical Chemistry,
Biochemistry and Biotechnology, University of Milan,
Milano, Italy

E. Costantino · A. Frattini · E. Caldana · A. Bettiga
Institute of Biomedical Technologies, CNR,
Milano, Italy

A. Frattini · E. Caldana
Institute Clinico Humanitas,
Rozzano, Italy

F. Rucci
Division of Immunology, Children's Hospital,
Harvard Medical School,
Boston, MA, USA

P. L. Poliani
Institute of Molecular Medicine, University of Brescia,
Brescia, Italy

A. Prinetti (✉)
Via Fratelli Cervi 93,
20090 Segrate, Milan, Italy
e-mail: alessandro.prinetti@unimi.it

In the last few years, cellular and molecular investigations of hereditary osteopetrosis have greatly contributed to the dissection of this heterogeneous disease.

Human osteopetrosis in most, but not all cases [2], shows normal or increased numbers of osteoclasts [1] and it has been suggested that the affected gene(s) is likely involved in the maintenance of the functional capacity of mature osteoclasts. This hypothesis has been supported by the nature of the gene defects found thus far in ARO osteoclast rich-form, all related to metabolic pathways leading to acidification of the external microenvironment. The a3 subunit (coded by ATP6a3 or TCIRG1 gene) of the V-ATPase complex, the primary pump involved in proton extrusion by osteoclast cells, has been found mutated in more than 60% of the patients affected by ARO [3–5]. This acidification is also been hampered by a defect in the ClCN7 gene, which is mutated in about 10% of ARO patients [6, 7]. This gene, whose mutations are also responsible for the Autosomal Dominant Osteopetrosis type II [8], encodes a late endosomal/lysosomal member of the CLC family of chloride channels and transporters [9].

A third gene mutated in human ARO is the grey-lethal gene (*gl*/*gl*), named OSTM1, (osteopetrosis associated transmembrane protein-1 which encodes a single transmembrane domain protein that has been suggested to form a molecular complex with ClC-7 [10]. The OSTM1 is responsible for the grey-lethal mutation in the mouse, and has been described so far in about 4% of ARO patients [10–14]. In addition it has been demonstrated that the OSTM1-dependent patients show seizure and severe central nervous system involvement leading to a more severe prognosis then in ClCN7-dependent form [14].

Careful genotype/phenotype correlations in ARO suggest that, although at a first glance ARO patients look monomorphous, at a closer examination the underlying specific molecular defect seems to be of some prognostic and therapeutic relevance. TCIRG1-dependent ARO patients have a severe homogeneous phenotype, their nervous system involvement (hydrocephalus and cranial nerve defects) is secondary to the compression due to skull deformities and the haematological defects can be rescued by HLA-matched haematopoietic stem cells (HSC) transplantation [15, 16].

On the other hand, there is increasing evidence that patients with recessive ClCN7 and OSTM1 mutations, besides the bone manifestations, show a primary severe neurological defect (primary retinopathy and progressive cortical atrophy in addition to secondary neural defects) due to lysosomal storage disease, as recently suggested [8].

It has been reported that ClC-7 and OSTM1 proteins co-localize in late endosomes and lysosomes of various cell type including neuronal cells, as well as in the ruffled border of bone-resorbing osteoclasts. ClC-7 and OSTM1 form a molecular complex with the OSTM1 as β-subunit of ClC-7 and mutations in either gene lead to lysosomal storage and neurodegeneration in addition to osteopetrosis [8]. These finding could explain why the prognosis of both of these forms seems particularly poor due to the co-existence of this neurological defect which leads to death in spite of HSCT [5, 6, 8, 15, 16], but doesn't explain the origin of the neurological involvement.

We have previously demonstrated that both human and the mouse mutant have a primary CNS involvement consisting of progressive cortical atrophy and hypomyelination/dysmyelination, suggesting that the grey-lethal mouse is a good model to investigate the role of this gene and to test possible alternative therapies [14].

Recently, a different role has been proposed for the OSTM1 protein. It has been demonstrated that, in totipotent mouse F9 embryonal teratocarcinoma, expression of wild type OSTM1 increases Wnt3a-responsive beta-catenin accumulation and Lef/Tcf-sensitive transcription and that expression of OSTM1 with a C-terminal deletion inhibited the Wnt-dependent association of beta-catenin and Lef1, suggesting that OSTM1 is involved in signaling of the Wnt/beta-catenin "canonical" pathway [17].

Preliminary data indicate that *gl*/*gl* mouse brain is smaller in size with irregular globose hemisphere and shows a diffuse translucent appearance with loss of the normal demarcation between the white and the grey matter, features consistent with myelin loss or hypomyelination/dysmyelination [14].

To better understand the nature of the neurological defects, we have analyzed the biochemistry as well as the pathology of the nervous system in the grey-lethal mutant mouse.

## Materials and methods

*Materials* Commercial chemicals were the purest available, common solvents were distilled before use, and water was prepared by the MilliQ system (Millipore). High performance silica gel precoated thin-layer plates (TLC Kiesegel 60) were purchased from Merck. Trypsin, crystalline bovine serum albumin, aminoacids and reagents for cell culture were purchased from Sigma-Aldrich Chemicals. Dulbecco's Modified Eagle's Medium (D-MEM) and fetal calf serum were purchased from Hy-Clone.

Sphingolipids to be used as standard were purchased from Sigma and the purity checked by thin layer chromatography in the appropriate solvent systems.

Isotopic tritium labeled gangliosides GM1 and GM2 were prepared by the dichloro-dicyano-benzoquinone/sodium boro[$^3$H]hydrid method followed by reversed phase HPLC purification [18, 19]. [3–$^3$H(*sphingosine*)]GM1 and [3–$^3$H

(*sphingosine*)]GM2, had a specific radioactivity of 1.2 and 1.1 Ci/mmol, respectively.

The mouse strains GL/Le *Edardl-J* were obtained from the Jackson Laboratory (Bar Harbor, ME). Homozygous *gl*/*gl* mice were obtained by breeding heterozygous mice with the mutated allele. Mice were maintained in accordance with Italian Ministry of Health and European Community guidelines, and the experimental procedures were in compliance with the guiding principles in the Guide for the Care and Use of Laboratory.

*Lipid extraction* Brains from *gl*/*gl* and wild type mice were weighted, frozen and lyophilised. The lyophilised tissue was suspended in iced water (500 mg of fresh tissue/ml), sonicated maintaining the sample tube in ice immersion, and again frozen and lyophilised. Lipids were extracted from the lyophilised powder (80 mg fresh tissue/ml) with chloroform/methanol/water, 20:10:1 (by volume) for three times [20]. Total lipid extracts were subjected to a two-phase partitioning [21, 22] resulting in the separation of an aqueous phase containing gangliosides and in an organic phase containing all other lipids. The aqueous phase ganglioside content was determined as lipid-bound sialic acid by the resorcinol method [23], while phospholipid content of the organic phase was determined as lipid-bound phosphate after perchloric acid digestion [24]. Lipids were separated by mono-dimensional TLC carried out with the following solvent systems: hexane/ethyl acetate, 3:2 by volume for the analysis of cholesterol, chloroform/methanol/acetic acid/water, 30:20:2:1 by volume for phospholipids, chloroform/methanol/0.2% aqueous $CaCl_2$, 50:42:11 by volume for gangliosides. The *O*-acetylated gangliosides were analysed by two-dimensional TLC carried out with chloroform/methanol/water, 50:42:11 by volume for the first and the second run and with intermediate exposure to $NH_3$ vapors. The solvent systems chloroform/methanol/water, 110:40:6 and 70:25:4 by volume were used to analyse, respectively, neutral glycolipids and sulfatide from organic phases after alkaline treatment [20]. Galactosylceramide and glucosylceramide were separated on borate impregnated TLC [25] with the solvent system chloroform/methanol/2.5 M ammonium hydroxide, 70:30:3 by volume. Identification of lipids after separation was assessed by co-migration with lipid standards.

Cholesterol was visualized by spraying the TLC with 15% concentrated sulphuric acid in 1-butanol [26], phospholipids with the molybdate reagent [27], gangliosides with the *p*-dimethylaminobenzaldehyde reagent [28], neutral glycolipids with the aniline/diphenylamine reagent [29] and sulfatide with the cresyl violet acetate reagent [30]. Lipid quantification was determined by densitometry after TLC separation using the Molecular Analyst program (Bio-Rad Laboratories, Hercules, CA, USA). The mass content of each phospholipid, or ganglioside, was calculated on the basis of the percentage distribution of total phospholipid, or ganglioside, content. Lipid contents were referred to brain weigh or to brain protein content determined according to Lowry [31], using bovine serum albumin as the reference standard.

The lipid composition of brains from three different animals from different litters has been analyzed. Data are the mean values±SD, statistical significance of the differences between *gl*/*gl* and wild type mice has been carried out using a two-tailed test. In some cases, the brains from littermate animals have been analysed, reporting the individual composition data.

*Enzyme assays* The lysosomal enzyme activities were determined utilizing the appropriate methyl-umbiferryl substrates on brain homogenates obtained from three animals from different litters for each day of age. Data are the mean values±SD, statistical significance of the differences between *gl*/*gl* and wild type mice has been carried out using a two-tailed test.

*Cell cultures* Fibroblasts were derived from wild type and *gl*/*gl* mouse skin were cultured in Dulbecco's Modified Eagle's Medium (D-MEM) containing 10% fetal bovine serum, non essential amino acid mixture, 100 units/ml penicillin, 100 μg/ml streptomycin, and 2 mM L-glutamine. Cells were maintained at 37°C in a humidified atmosphere containing 5% $CO_2$.

The viability of the cells was estimated by examining their ability to exclude 0.1% trypan blue in 0.9% NaCl.

*Feeding experiments* [3–$^3$H(*sphingosine*)]GM1 and [3–$^3$H(*sphingosine*)]GM2, dissolved in propan-1-ol/water, 7:3 by volume, were pipetted into a sterile tube and dried under a nitrogen stream. The residue was solubilized in an appropriate volume of pre-warmed (37°C) Dulbecco's Modified Eagle's Medium (D-MEM), to obtain a 1.25 μM solution. After removal of the original medium and rapid washing of cells with D-MEM without serum, 5 ml of the medium without serum and containing the radioactive lipid were added to each dish of normal and *gl*/*gl* fibroblasts. Cells were incubated for 4 h at 37°C, the radioactive medium was removed and the dishes were washed with D-MEM with 10% serum and chased for 19 h with 10% FCS D-MEM. After chase, cells were washed twice with 5 ml of D-MEM, scraped off with PBS with $Na_4VO_4$ by a rubber policeman and centrifuged at 3,000 rpm for 10 min at 4°C. The cell pellets were submitted to lipids extraction and lipid analyses as reported above. Radioactive lipids were separated by TLC as reported above and subjected to radio-imaging with a Beta-Imager 2000 instrument (Biospace, Paris).

*Histopathological analysis* At time of sacrifice, all mice were deeply anesthetized and perfused with 4% paraformaldehyde. Brains and spinal cords were removed and post-fixed o.n. in the same fixative prior to paraffin embedding following a routine protocol. 4 μm tissue sections were taken on a microtome and used for routine Haematoxylin and Eosin (H&E) staining and immunohistochemistry. Briefly, sections were de-waxed, re-hydratated through serial passages in xylene and alcohol and endogenous peroxidase activity blocked with 0.3% H2O2 in methanol. Sections were washed again and incubated 20 min. in 5% normal serum from the "secondary antibody species and over night with the primary monoclonal antibody mouse anti-2′, 3′-cyclic nucleotide 3′-phosphodiesterase (CNPase, 1:1,000; Sigma, St Louis, MO, USA). After washing, slides were incubated 1 h in the secondary goat anti-mouse biotin-labelled antibody (1:200; Dako Cytomation) and signal revealed by peroxidase conjugated streptavidin (HRP, 1:20; BioGenex, S. Ramon, CA, USA) and diaminobenzydine (DAB, 1:50; BioGenex). Slides were then counterstained with Hematoxylin. Negative controls were obtained by omitting primary or secondary antibodies, respectively. Images were acquired with the Olympus DP70 digital camera mounted on an Olympus BX60 microscope using the Olympus imaging software Cell^F 2.5.

## Results

The spontaneous *grey-lethal* (*gl*/*gl*) mouse model perfectly recapitulates the severe OSTM1 human malignant autosomal recessive form of osteopetrosis [32]. Osteopetrosis in homozygous *gl*/*gl* mice is fully penetrant and can be rescued by bone marrow transplantation providing evidence of a cell-autonomous defect [33].

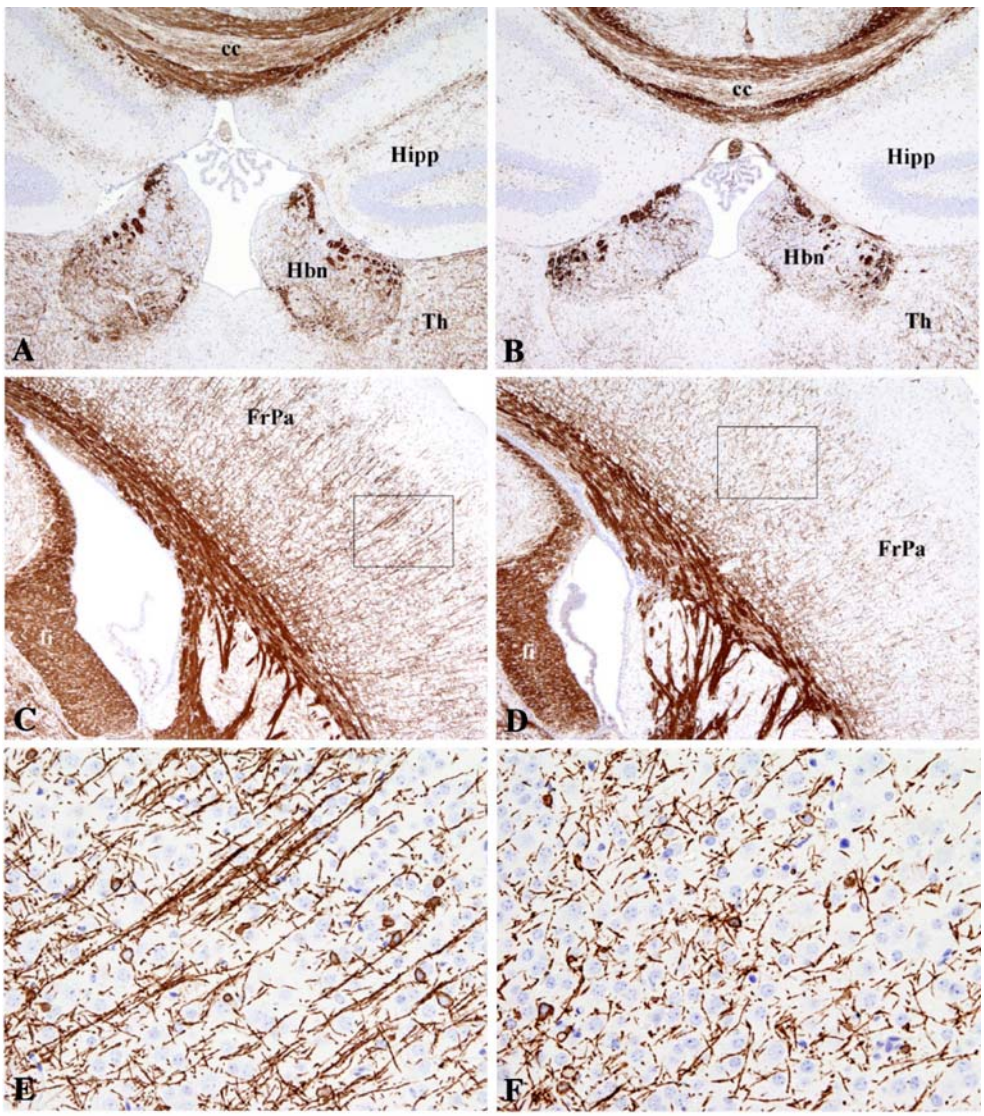


**Fig. 1** Reduction of myelin fibres in the grey-lethal (*gl*/*gl*) mouse brain compared with the wild type (+/+). CNPase immunostaining highlights normal myelin distribution and oligodendrocytes number in the brain of a 2 weeks old wild type mouse (**a**, **c** and **e**) compare to the age-matched *gl*/*gl* mouse brain (**b**, **d** and **f**). Corpus callosum from the *gl*/*gl* mouse brain show a severe loss of myelin fibres (**b**) as compared to the control mouse brain (**a**). Cortical regions show rarefaction of the distribution in myelin fibres (**d**) compare to the control (**c**). Details of the cortical regions shown in **c** and **d** highlight loss of both oligodendrocytes and myelinated fibers in the *gl*/*gl* mice (**d**) compare to the controls (**c**). **a**, **b**, **c** and **d** are from 4× and **e** and **f** from 20× original magnification. *CC* Corpus callosum, *Hbn* habenular nucleus, *Th* thalamus (partial), *Hipp* hippocampus. Images are representative of those obtained analyzing three different animals

**Table 1** Protein, ganglioside, cholesterol and glycerophospholipid contents in the brains from wild type and grey-lethal (*gl*/*gl*) mice, at different age

| Age, days | Proteins, mg/g wet brain | | Gangliosides, μg sialic acid/g wet brain | | Cholesterol, mg/g wet brain | | Glycerophospholipids, μmol phosphorus/g wet brain | |
|---|---|---|---|---|---|---|---|---|
| | WT | *gl*/*gl* | WT | *gl*/*gl* | WT | *gl*/*gl* | WT | *gl*/*gl* |
| 8 | 78.25±7.61 | 80.02±7.68 | 652±58 | 663±49 | 5.6±0.5 | 5.2±0.5 | 27.9±3.0 | 25.4±2.2 |
| 10 | | 88.04±8.65 | | 805±65 | | 6.6±0.6 | | 32.0±2.0 |
| 11 | | 76.87±6.71 | | 788±69 | | 4.7±0.3 | | 32.8±2.1 |
| 12 | 82.13±7.54 | 73.78±6.63 | 694±58 | 720±71 | 6.6±0.5 | 5.8±0.6 | 36.0±1.9 | 33.0±3.1 |
| 13 | | 85.21±8.88 | | 820±79 | | 5.8±0.5 | | 35.0±2.3 |
| 14 | 81.03±7.91 | 82.13±6.69 | 623±60 | 633±59 | 4.4±0.5 | 4.8±0.6 | 29.5±2.1 | 29.7±2.8 |
| 15 | 75.03±5.94 | 79.14±6.12 | 670±58 | *741±51 | 5.9±0.4 | 7.0±0.6 | 40.3±3.2 | 40.2±2.9 |
| 19 | 83.35±6.61 | 86.33±7.01 | 717±60 | *784±62 | 6.9±0.6 | 6.8±0.5 | 36.4±3.4 | 41.0±3.9 |
| 20 | | 77.15±7.02 | | 936±91 | | 6.1±0.7 | | 40.8±3.7 |
| 21 | | 83.22±6.99 | | 1007±93 | | 5.8±0.6 | | 44.3±2.9 |

The lipid composition of brains from three different animals from different litters has been analyzed. Data are the mean values±SD, statistical significance of the differences between *gl*/*gl* and wild type mice has been carried out using a two-tailed test
*$P<0.01$ vs age-matched wild type mice

Homozygous *gl*/*gl* mice do not display tooth eruption, due to loss of bone remodelling and show a characteristic grey coat colour instead of agouti as a consequence of pheomelanin granules clumping in melanocytes.

The affected mice show bone sclerosis, mild anemia and pancytopenia, developmental delay, blindness, dysmyelination mainly at the level of the corpus callosum, cortical dysplasia. Death occurs within 2–3 weeks of age presumably due to neurological defect.

The spontaneous *grey-lethal* mutation consists of a 1.5 kb genomic deletion encompassing the 5′ region of the OSTM1 gene. Consequently, the transcript and protein

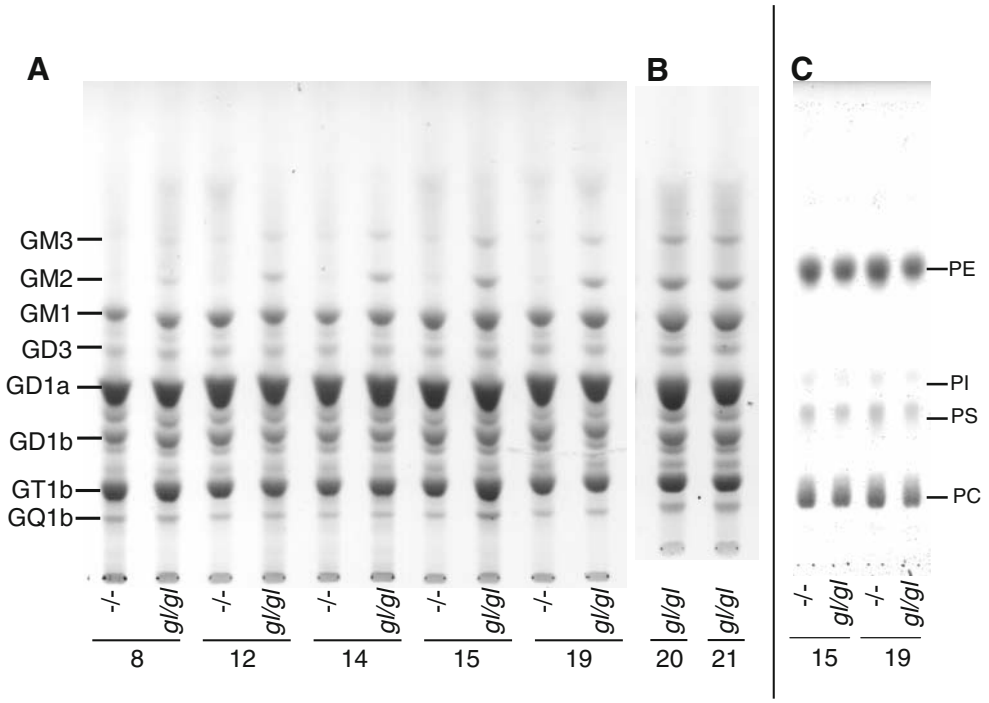


**Fig. 2** TLC separation of the complex lipids from wild type and grey-lethal mouse (*gl*/*gl*) brains. The total lipid mixture from wild type and grey-lethal mouse (*gl*/*gl*) brains was partitioned in aqueous and organic phases that were analysed separately. **a** and **b** The TLC separation of the aqueous phase ganglioside mixture from the brain of mice at different age, in days. Gangliosides were separated with the solvent system chloroform-methanol-0.2% aqueous $CaCl_2$, 50:42:11 by volume and visualized with the *p*-dimethylaminobenzaldehyde reagent. The ganglioside mixtures from the brains of grey-lethal mice at day 20 and 21 were analysed on a separate plate (**b**). **c** The organic phase glycerophospholipid mixtures. Glycerophospholipids were separated with the solvent system chloroform/methanol/acetic acid/water, 30:20:2:1 by volume and visualized with the molybdate reagent. TLC patterns are representative of those obtained analyzing brains from three different animals

are completely undetectable in homozygous *gl*/*gl* mice. The OSTM1 protein contains a putative signal peptide at the N-terminal end and one membrane spanning domain in the C-terminal region [11].

In wt tissue, OSTM1 is highly expressed in osteoclasts and melanocytes, consistent with the phenotype observed in *gl*/*gl* animals and moderate express in brain, spleen and kidney tissues, where the protein may have a crucial function.

*Myelination in the gl/gl mouse* Gross examination of the brain indicated that in the *gl*/*gl* normal demarcation between the white and the grey matter is absent. Histological analysis showed loss of normal lamination in cortex consistent with multiple foci of cortical dysplasia.

Preliminary immunohistochemical analysis showed hypomyelination/dysmyelination at the level of the corpus callosum [13].

We have now performed a more detailed analysis of the myelin abnormalities present at P14 in mutant brain by immunostaining myelin and oligodendrocytes with anti-CNPase antibodies. The results of our studies show that in the mutants, compared to wild type mice the myelin deficit is extensive (Fig. 1), myelinated fibers and oligodendrocytes in the *gl*/*gl* brain are completely absent around the hippocampal area, and significantly reduced in thalamus, habenula (Fig. 1a–b) as well as in the cerebral cortex (Fig. 1c–d). Higher magnification of the parietal cortex (enclosed in the insert) shows significant abnormalities of the myelinated fibres. In the wt brain the fibers are well myelinated (Fig. 1e) while in the *gl*/*gl* they appear to be disorganized and fragmented (Fig. 1f). No significant difference are appreciated in morphology of oligodendrocytes between mutants and wild type controls.

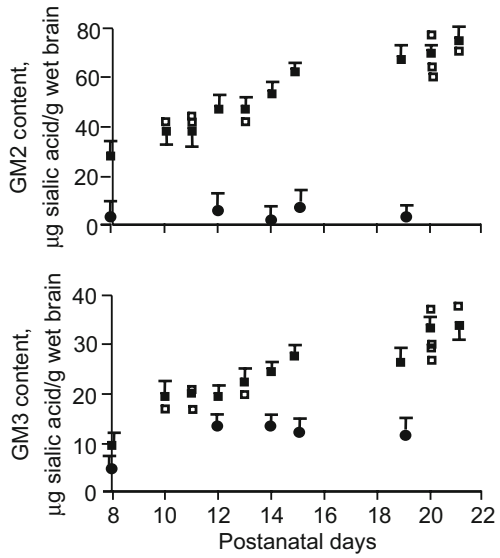


**Fig. 3** GM2 and GM3 contents in the brains from wild type and grey-lethal (*gl*/*gl*) mice. The aqueous phase ganglioside mixtures were separated by TLC as in Fig. 2, and each spot quantified by densitometry. Percentage values were then converted into absolute values on the basis of total ganglioside sialic acid content. *Circles* represent gangliosides from wild type brains; the *closed squares* represent gangliosides from the brains of grey-lethal mice from different litters, *open squares* represent gangliosides from the brains of grey-lethal mice from the same litter. Data are the mean values± SD. In some cases, the brains from littermate animals have been analysed, reporting the individual composition data

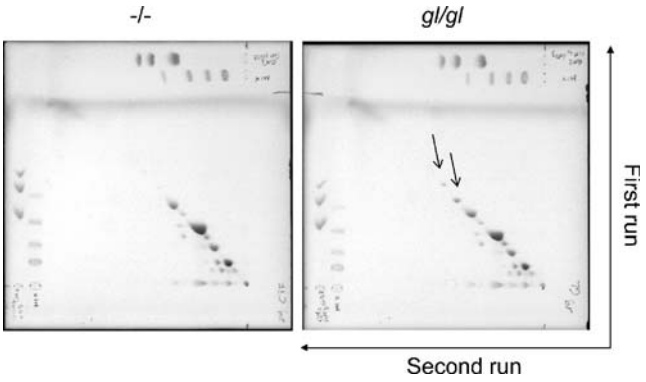


**Fig. 4** Two-dimensional TLC with intermediate ammonia treatment of the aqueous phase ganglioside mixture from the brains of 19 day old wild type and grey-lethal mice (*gl*/*gl*). The ganglioside mixtures were applied on the left side of the plate as a small circle. After the first run with the solvent system chloroform-methanol-0.2% aqueous $CaCl_2$, 50:42:11 by volume, the plate was dried, exposed to ammonia vapours to remove alkali labile linkages, rotated 90° and developed with the same above solvent system. Gangliosides were visualized with the *p*-dimethylaminobenzaldehyde reagent and alkali labile gangliosides are recognised as the spots under the diagonal of alkali labile gangliosides

*Alteration in the levels of myelin specific sphingolipids and complex lipids in brain of gl/gl during development* In order to correlate morphological abnormalities to metabolic events taking place during development we have analysed the content of the myelin specific lipids: galactosylceramides and sulfatides in the brain of wt and *gl*/*gl*. The accumulation, during development, of sphingomyelin, another sphingolipid highly enriched in the myelin membrane was also determined. To complete the analysis, the content and pattern of gangliosides, glycerophospholipids and cholesterol were investigated. The time frame of our experimental design, due to the short life span of the mutants, covers only from 8 to 21 days, nonetheless this is the period of most rapid myelination.

Both glycerophospholipid and cholesterol contents were not significantly different in *gl*/*gl* and wild type mice (Table 1). In addition, no significant differences were found in the glycerophospholipid patterns (Fig. 2c).

However, deep differences were observed in the sphingolipid composition of the *gl*/*gl* mouse brain. Figure 2a,b, shows the monodimensional HPTLC separation of the brain ganglioside mixture from 8 to 21 day old mice. In

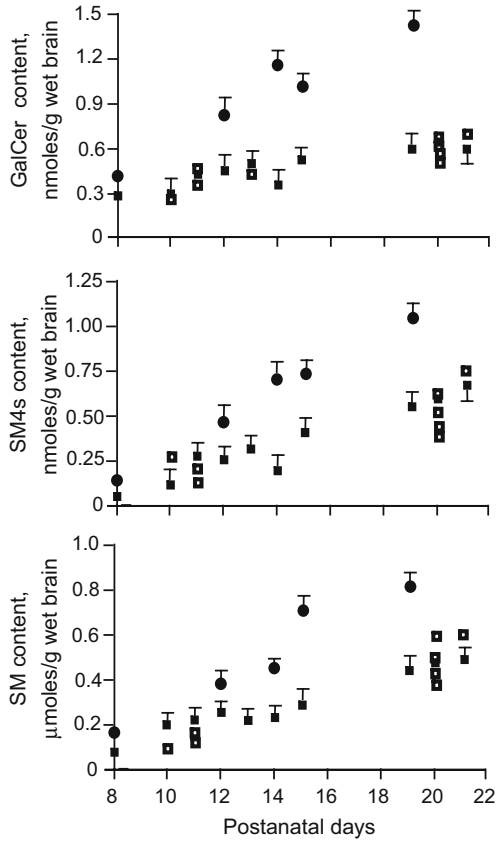


**Fig. 5** Galactosylceramide, sulfatide and sphingomyelin contents in the brains from wild type and grey-lethal (*gl*/*gl*) mice.The galactosylceramide (*upper panel*), sulfatide (*middle panel*) and sphingomyelin (*lower panel*) contents were determined in the organic phase after alkaline treatment to remove glycerophospholipids. The organic phase was separated with different solvent systems as reported in the experimental section. Sphingolipids were quantified by densitometry by comparison with known quantities of reference standards. *Circles* represent sphingolipids from wild type brains; the *closed squares* represent sphingolipids from the brains of grey-lethal mice from different litters, *open squares* represent sphingolipids from the brains of grey-lethal mice from the same litter. Data are the mean values±SD. In some cases, the brains from littermate animals have been analysed, reporting the individual composition data

agreement with previous data [34] the brain ganglioside mixture of wild type mice showed a mild increase as total sialic acid within the age range (Table 1). The ganglioside content in *gl*/*gl* brains was very similar to that of wild type mouse brains at day 8, while in 15 and 19 day old mice it was slightly (about 10%) but significantly higher than in wild type mouse brains. Analysis of ganglioside pattern in the brains from *gl*/*gl* mice from 8 to 21 day old mice showed a progressive percentage increase of the two monosialogangliosides GM3 and GM2. The content of these two gangliosides was responsible for the higher total ganglioside sialic acid content in *gl*/*gl* brains with respect to wild type mouse brains. Figure 3 shows the changes of gangliosides GM3 and GM2 contents in the brains from wild type and grey-lethal mice along aging. As expected both GM3 and GM2 are very minor components of the total ganglioside mixture from the brains of wild type mice, comprising for a few micrograms of sialic acid per g of wet brain. Instead, in the brains from *gl*/*gl* mice both gangliosides progressively increased along age becoming main components, particularly GM2, of the total ganglioside mixture. To analyze with a better resolution the ganglioside patterns in *gl*/*gl* and wild type mouse brain, we performed a two-dimensional TLC separation with intermediate ammonia treatment of the ganglioside mixtures. Figure 4 shows the two-dimensional TLC separation of the brain ganglioside mixtures from the 19 day old *gl*/*gl* and wild type mice. The chromatographic procedure allowed to recognize alkali labile gangliosides, namely *O*-acetylated sialic acid containing gangliosides and ganglioside-lactones. The accumulation of GM3 and GM2 is evident in the grey lethal brain, but no other significant differences were observed for both alkali-labile and alkali-stabile species between the two two-dimensional ganglioside patterns.

Galactosylceramide, sulfatide and sphingomyelin are sphingolipids typically enriched in myelin. Since histochemical analysis of brain suggested a demyelination process in grey lethal mice, we analysed in detail the galactosylceramde, sulfatide and sphingomyelin contents in grey lethal brains. Figure 5 shows the galactosylceramide

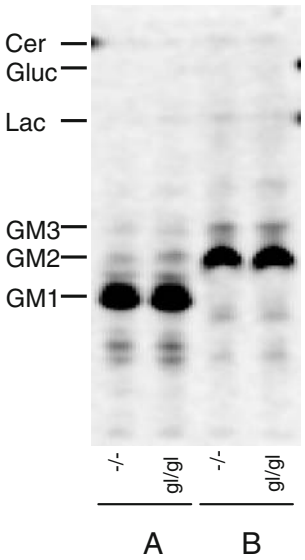


**Fig. 6** TLC separation of total radioactive lipid pattern from wild type and grey-lethal (*gl*/*gl*) fibroblasts fed with 3–$^{3}$H(*sphingosine*)]GM1 and [3–$^{3}$H(*sphingosine*)]GM2, in culture. Fibroblasts were fed for 4 h with [3–$^{3}$H(*sphingosine*)]GM1 and [3–$^{3}$H(*sphingosine*)]GM2 and after 19 h-chase, lipids were extracted and the total mixture separated by HPTLC using the solvent system chloroform/methanol/0.2% aqueous CaCl2, 50:45:10 by volume. Radioactive lipids were detected by digital autoradiography; 200–400 dpm were applied on a 4 mm line; time of acquisition: 24 h. *Lane A* Cells fed with [3–$^{3}$H(*sphingosine*)]GM1 *lane B*, cells fed with [3–$^{3}$H(*sphingosine*)]GM2. Patterns are representative of those obtained in two independent experiments

**Table 2** Enzyme activity in the brain homogenates from 8 and 23 day old wild type and grey-lethal mice (*gl*/*gl*)

| Enzyme | Substrate | Enzyme activity, nmol/mg protein/h | | | |
|---|---|---|---|---|---|
| | | WT | | *gl*/*gl* | |
| | | 8 day old | 23 day old | 8 day old | 23 day old |
| β-Hexosaminidase | MU-β-GalNAc | 12.47±1.51 | 24.79±1.98 | 33.27±2.11 | 37.25±3.21 |
| β-Hexosaminidase | MU-β-GalNAc-SO3 | 0.52±0.05 | 1.07±0.07 | *1.42±0.09 | *1.30±0.08 |
| β-Galattosidase | MU-β-Gal | 0.13±0.01 | 0.47±0.02 | *0.39±0.01 | 0.53±0.01 |
| α-Mannosidase | MU-α-Man | 0.51±0.02 | 0.52±0.02 | *2.09±0.05 | **3.60±0.04 |
| α-Fucosidase | MU-α-Fuc | 0.15±0.01 | 0.19±0.01 | *0.40±0.01 | *0.40±0.02 |

Brain homogenates from three different animals from different litters has been analyzed. Data are the mean values±SD, statistical significance of the differences between *gl*/*gl* and wild type mice has been carried out using a two-tailed test
*MU* Methylumbellyferyl group
*$P<0.01$, **$P<0.001$ vs age-matched wild type mice

(upper panel), sulfatide (middle panel) and (lower panel) sphingomyelin changes in *gl*/*gl* and wild type mouse brains along aging. The contents of these three sphingolipids were strongly (about 50%) reduced in the *gl*/*gl* brains with comparison with the wild type mouse brains, confirming the presence of a myelin damage in the mutant animals.

*Loading of labelled GM1 and GM2 in fibroblast of mutant and control fibroblasts* Accumulation of brain gangliosides is often the result of impairment of lysosomes due to defects of hydrolytic enzymes. Thus, we prepared cultures of skin fibroblasts from 19 day old *gl*/*gl* and wild type mice, and assessed their ability to catabolise gangliosides at the lysosomal level. Cultured fibroblasts are easily prepared and have proven to be a valuable tool to understand the basic metabolic defects underlying sphingolipid-storage diseases [35–37]. To do this, we fed fibroblasts in culture ganglioside tritium-labelled at the sphingosine moiety, to recognize the lysosomal degradation of gangliosides taken up by the cells and thus a possible lysosomal impairment occurring in the mutant mouse. In detail, fibroblasts from *gl*/*gl* and wild type mice were fed with GM1 to observe a possible accumulation of GM2, and were fed with GM2 to observe a possible accumulation of GM3. Figure 6 shows that gangliosides were taken up by the cells, partially metabolized to more complex gangliosides and partially catabolised to less complex glycosphingolipids. Nevertheless, the metabolic processes were comparable in *gl*/*gl* and wild type fibroblasts and no accumulation of gangliosides could be observed in *gl*/*gl* cells. In further experiments performed to study catabolism properties, we analysed the enzyme activity of some lysosomal hydrolases, namely β-hexosaminidase, β-galactosidase, α-mannosidase and α-fucosidase (Table 2). Enzyme activity was determined using the brain homogenates from 8 and 23 day old wild type and *gl*/*gl* mice on artificial substrates. We found that all the enzyme activities were higher in the brain homogenate from *gl*/*gl* and that the higher activities were observed yet in the 8 day old mice.

## Discussion

Human forms of autosomal recessive osteopetrosis associated with mutations of the grey-lethal gene (*gl*) encoding for OSTM1 are particularly severe and are characterized by a deep neural involvement, mainly consisting in progressive cortical atrophy associated with myelin damage [14]. The animal model of the disease, the spontaneous *gl*/*gl* mouse mutant, is also characterized by blindness and a marked neural impairment: It was previously described that *gl*/*gl* mouse shows reduced brain size with loss of the normal demarcation between the white and the grey matter. On histological examination, diffuse loss of myelin, mainly at the level of the corpus callosum, and cortical dysplasia were evidentiated. The early death of the animals is most likely due to the neurological defects. Our data clearly show that *gl*/*gl* cortex at P14 is characterized by evident signs of myelin deficit, including generalized dysmyelinogenesis. However, in evaluating the results of our studies concerning the lack of galactosylceramide accumulation during brain development, and given that galactolipids are critical early mediators of myelin formation, it is reasonable to conclude that hypomyelination is cause of the myelin deficit observed in the *gl*/*gl* brain. However, at this time and with the data available we cannot conclude whether the observed myelin alterations are the consequence of primary alterations in oligodendrocyte metabolism or secondary to neuronal pathology.

Neurologic involvement is a common feature of a vast group of clinically heterogeneous diseases belonging to lysosomal storage disorders. All lysosomal storage disorders are characterized by the genetically determined deficiency of a lysosomal catabolic enzyme [38], In particular, several

lysosomal storage diseases are characterized by defects in the lysosomal degradation pathways of complex sphingolipids [39], with the consequent accumulation of non degraded sphingolipids at the lysosomal level. All sphingolipid storage diseases are autosomal recessive diseases as human ARO. Among other sphingolipid storage diseases, phenotypes associated with neurological impairment are particularly evident in GM2 gangliosidosis (Sandhoff and Tay-Sachs diseases), Niemann-Pick disease type A, Gaucher disease, metachromatic leukodistrophy and globoid cell leukodistrophy (Krabbe disease).

In some cases, within the same pathology are present both neuronopathic and non neuronopathic forms. In other cases, a myelin defect is the primary event, such as in Krabbe disease, an inflammatory demyelinating disease caused by genetic deficiency of the galactosylceramidase, that leads to the accumulation of galactosylsphingosine, one of the substrates of galactosylceramidase.

Accumulation of galactosyl sphingosine, a toxic compound, is the cause for the apoptotic death of myelin-producing olygodendrocytes and the infiltration of periodic acid Schiff stain-positive peripheral macrophages, leading to extensive demyelination [40, 41].

Sphingolipids are characteristic components of the plasma membrane of primary importance as receptors and cell surface antigens [42]. Moreover, cell sphingolipids contribute to the modulation of several cellular functions due to the ability to interact with specific proteins at the cell surface, and to modulate their functional activity. Indeed, the spontaneous segregation of membrane sphingolipids is the driving force leading to the creation of sphingolipid-enriched membrane domains or lipid rafts, where a highly selected set of lipids and proteins are segregated together, allowing reciprocal interactions of functional significance and forming functional units which are involved in signal transduction processes. When lysosomes are overloaded by the excess of non-degradable sphingolipids, a certain amount of the accumulated sphingolipid can be transported to the plasma membrane and to intracellular membranes, thus modifying their composition and leading to relevant modifications in the structure of lipid rafts and in the interactions occurring there between sphingolipids and proteins resident in lipid rafts. Moreover, lysosomal membranes are able to recycle to the plasma membrane, thus influencing its composition in an aberrant way in the case of lysosome degeneration [43]. The interaction with lipid membrane domains having non-conventional organization might deeply influence the interactions between sphingolipids and proteins at this level, influencing their function and participating to the onset of the neurodegenerative processes. More specifically, a possible role of lipid rafts in the pathogenesis of spontaneous and transmissible neurodegenerative diseases was highlighted by the discovery that a number of molecules causally connected to such diseases are associated with these membrane domains. The most prominent examples are represented by the amyloid precursor protein (APP) in Alzheimer's disease [44–47] or synuclein in Parkinson disease [48, 49] and by the prion protein [50]. In both cases, the generation of the aberrant forms of these proteins, which are responsible for the onset of the disease, seems to be localized in lipid rafts and/or dependent from the structure of lipid rafts.

For these reasons, we analyzed the brain lipid composition of *gl*/*gl* mice at different ages and compared to that of wild type mice. Our data have clearly shown a lack of cumulative increase of sphingomyelin, sulfatide and galactosylceramide during development in the brain of *gl*/*gl* compared to controls. Since myelin is highly enriched in these three sphingolipids, these results are consistent with the immunohistochemical data indicating a depletion of myelinated fibers in the brain of *gl*/*gl* mice. On the other hand, we observed in *gl*/*gl* mouse brain a progressive accumulation of the monosialogangliosides GM3 and GM2. Thus, we wondered whether the myelin alterations could be the consequence of the accumulation of these gangliosides as the result of a defect of their degradation. Thus, we analyzed the enzyme activities of several lysosomal glycohydrolases. Surprisingly, we found that all enzyme activities tested were higher or similar in the *gl*/*gl* mice brain homogenates respect to the wild type animals. Moreover, we tested the ability of cultured skin fibroblasts from wild type and grey lethal mice for their ability to catabolize exogenously added gangliosides, and no difference were observed in the uptake and catabolism of exogenous GM1 and GM2, nor accumulation of products deriving from the catabolism of gangliosides. Thus, the metabolic origin of the accumulation of GM3 and GM2 in *gl*/*gl* mice brain remains to be elucidated. It is worth to recall that accumulation of gangliosides in brain areas has been observed in the case of human Niemann-Pick disease type A, that is consequent to the lack of acidic sphingomyelinase and accumulation of sphingomyelin [51], indicating that a specific enzyme defect in sphingolipid catabolism might lead to unexpected consequences on the tissue levels of sphingolipids that are not the direct substrate of the defective enzyme. Since our data seem to rule out the involvement of enzymes of ganglioside degradative pathway in determining the accumulation of monosialogangliosides in *gl*/*gl* mouse brain, it is likely that altered glycolipids glycosylation could be responsible for this. We are currently testing this hypothesis by comparatively analyzing the expression levels and enzyme activities of different glycolipid glycosyltransferases in wild type and *gl*/*gl* mouse brain. It is well known that genes encoding for glycolipid glycosyltransferases are under transcriptional control [52]. The synthetic reactions leading to the stepwise addition of sugars during glycolipid biosynthesis are

coupled to vesicular transport in the Golgi apparatus [53], and different acceptors compete for the enzyme activities at the branching point of the biosynthetic pathway, that thus represent a potential site of regulation for ganglioside biosynthesis. Moreover, glycosyltransferases for glycolipids are organized as multimolecular complexes in the Golgi [54]. Thus many factors affecting the organization and traffic in intracellular membranes could be responsible for an altered glycosylation leading to the observed accumulation of GM3 and GM2 gangliosides in *gl*/*gl* mouse brain. It remain to be elucidated whether this occurs in this experimental model of ARO.

A possible clue to understand the molecular basis of the pathological features described in this paper will come from a detailed analysis of the neuronal compartment. An important goal will be understand how the OSTM1 influences the neuronal activity and how its loss of function perturbs the neuron-oligodendrocyte interaction.

**Acknowledgements** This work was supported by University of Milan (FIRST to S.S.), CARIPLO Foundation (to S.S.) and by Mitzutani Foundation for Glycoscience (to A.P.).

## References

1. Tolar, J., Teitelbaum, S.L., Orchard, P.J.: Osteopetrosis. N. Engl. J. Med. **351**, 2839–2849 (2004). doi:10.1056/NEJMra040952
2. Sobacchi, C., Frattini, A., Guerrini, M.M., Abinun, M., Pangrazio, A., Susani, L., *et al.*: Osteoclast-poor human osteopetrosis due to mutations in the gene encoding RANKL. Nat. Genet. **39**, 960–962 (2007). doi:10.1038/ng2076
3. Frattini, A., Orchard, P.J., Sobacchi, C., Giliani, S., Abinun, M., Mattsson, J.P., *et al.*: Defects in TCIRG1 subunit of the vacuolar proton pump are responsible for a subset of human autosomal recessive osteopetrosis. Nat. Genet. **25**, 343–346 (2000). doi:10.1038/77131
4. Kornak, U., Schulz, A., Friedrich, W., Uhlhaas, S., Kremens, B., Voit, T., *et al.*: Mutations in the a3 subunit of the vacuolar H(+)-ATPase cause infantile malignant osteopetrosis. Hum. Mol. Genet. **9**, 2059–2063 (2000). doi:10.1093/hmg/9.13.2059
5. Scimeca, J.C., Quincey, D., Parrinello, H., Romatet, D., Grosgeorge, J., Gaudray, P., *et al.*: Novel mutations in the TCIRG1 gene encoding the a3 subunit of the vacuolar proton pump in patients affected by infantile malignant osteopetrosis. Hum. Mutat. **21**, 151–157 (2003). doi:10.1002/humu.10165
6. Frattini, A., Pangrazio, A., Susani, L., Sobacchi, C., Mirolo, M., Abinun, M., *et al.*: Chloride schannel ClCN7 mutations are responsible for severe recessive, dominant, and intermediate osteopetrosis. J. Bone Miner. Res. **18**, 1740–1747 (2003). doi:10.1359/jbmr.2003.18.10.1740
7. Kornak, U., Kasper, D., Bosl, M.R., Kaiser, E., Schweizer, M., Schulz, A., *et al.*: Loss of the ClC-7 chloride channel leads to osteopetrosis in mice and man. Cell **104**, 205–215 (2001). doi:10.1016/S0092-8674(01)00206-9
8. Cleiren, E., Benichou, O., Van Hul, E., Gram, J., Bollerslev, J., Singer, F.R., *et al.*: Albers-Schonberg disease (autosomal dominant osteopetrosis, type II) results from mutations in the ClCN7 chloride channel gene. Hum. Mol. Genet. **10**, 2861–2867 (2001). doi:10.1093/hmg/10.25.2861
9. Lange, P.F., Wartosch, L., Jentsch, T.J., Fuhrmann, J.C.: ClC-7 requires Ostm1 as a beta-subunit to support bone resorption and lysosomal function. Nature **440**, 220–223 (2006). doi:10.1038/nature04535
10. Jentsch, T.J.: Chloride and the endosomal-lysosomal pathway: emerging roles of CLC chloride transporters. J. Physiol. **578**, 633–640 (2007). doi:10.1113/jphysiol.2006.124719
11. Chalhoub, N., Benachenhou, N., Rajapurohitam, V., Pata, M., Ferron, M., Frattini, A., *et al.*: Grey-lethal mutation induces severe malignant autosomal recessive osteopetrosis in mouse and human. Nat. Med. **9**, 399–406 (2003). doi:10.1038/nm842
12. Quarello, P., Forni, M., Barberis, L., Defilippi, C., Campagnoli, M.F., Silvestro, L., *et al.*: Severe malignant osteopetrosis caused by a GL gene mutation. J. Bone Miner. Res. **19**, 1194–1199 (2004). doi:10.1359/JBMR.040407
13. Ramirez, A., Faupel, J., Goebel, I., Stiller, A., Beyer, S., Stockle, C., *et al.*: Identification of a novel mutation in the coding region of the grey-lethal gene OSTM1 in human malignant infantile osteopetrosis. Hum. Mutat. **23**, 471–476 (2004). doi:10.1002/humu.20028
14. Pangrazio, A., Poliani, P.L., Megarbane, A., Lefranc, G., Lanino, E., Di Rocco, M., *et al.*: Mutations in OSTM1 (grey lethal) define a particularly severe form of autosomal recessive osteopetrosis with neural involvement. J. Bone Miner. Res. **21**, 1098–1105 (2006). doi:10.1359/jbmr.060403
15. Gerritsen, E.J., Vossen, J.M., Fasth, A., Friedrich, W., Morgan, G., Padmos, A., *et al.*: Bone marrow transplantation for autosomal recessive osteopetrosis. A report from the Working Party on Inborn Errors of the European Bone Marrow Transplantation Group. J. Pediatr. **125**, 896–902 (1994). doi:10.1016/S0022-3476(05)82004-9
16. Driessen, G.J., Gerritsen, E.J., Fischer, A., Fasth, A., Hop, W.C., Veys, P., *et al.*: Long-term outcome of haematopoietic stem cell transplantation in autosomal recessive osteopetrosis: an EBMT report. Bone Marrow Transplant. **32**, 657–663 (2003). doi:10.1038/sj.bmt.1704194
17. Feigin, M.E., Malbon, C.C.: OSTM1 regulates beta-catenin/Lef1 interaction and is required for Wnt/beta-catenin signaling. Cell. Signal. **20**, 949–957 (2008). doi:10.1016/j.cellsig.2008.01.009
18. Ghidoni, R., Sonnino, S., Masserini, M., Orlando, P., Tettamanti, G.: Specific tritium labeling of gangliosides at the 3-position of sphingosines. J. Lipid Res. **22**, 1286–1295 (1981)
19. Negroni, E., Chigorno, V., Tettamanti, G., Sonnino, S.: Evaluation of the efficiency of an assay procedure for gangliosides in human serum. Glycoconj. J. **13**, 347–352 (1996). doi:10.1007/BF00731466
20. Prinetti, A., Chigorno, V., Prioni, S., Loberto, N., Marano, N., Tettamanti, G., *et al.*: Changes in the lipid turnover, composition, and organization, as sphingolipid-enriched membrane domains, in rat cerebellar granule cells developing in vitro. J. Biol. Chem. **276**, 21136–21145 (2001). doi:10.1074/jbc.M010666200
21. Riboni, L., Bassi, R., Sonnino, S., Tettamanti, G.: Formation of free sphingosine and ceramide from exogenous ganglioside GM1 by cerebellar granule cells in culture. FEBS Lett. **300**, 188–192 (1992). doi:10.1016/0014-5793(92)80193-K
22. Riboni, L., Prinetti, A., Pitto, M., Tettamanti, G.: Patterns of endogenous gangliosides and metabolic processing of exogenous gangliosides in cerebellar granule cells during differentiation in culture. Neurochem. Res. **15**, 1175–1183 (1990). doi:10.1007/BF01208577
23. Svennerholm, L.: Quantitative estimation of sialic acids. II. A colorimetric resorcinol-hydrochloric acid method. Biochim. Biophys. Acta **24**, 604–611 (1957). doi:10.1016/0006-3002(57)90254-8
24. Bartlett, G.R.: Phosphorus assay in column chromatography. J. Biol. Chem. **234**, 466–468 (1959)

25. Kean, E.L.: Separation of gluco- and galactocerebrosides by means of borate thin-layer chromatography. J. Lipid Res. **7**, 449–452 (1966)
26. Prinetti, A., Chigorno, V., Tettamanti, G., Sonnino, S.: Sphingolipid-enriched membrane domains from rat cerebellar granule cells differentiated in culture. A compositional study. J. Biol. Chem. **275**, 11658–11665 (2000). doi:10.1074/jbc.275.16.11658
27. Vaskovsky, V.E., Kostetsky, E.Y.: Modified spray for the detection of phospholipids on thin-layer chromatograms. J. Lipid Res. **9**, 396 (1968)
28. Partridge, S.M.: Filter-paper partition chromatography of sugars: 1. General description and application to the qualitative analysis of sugars in apple juice, egg white and foetal blood of sheep. with a note by R. G. Westall. Biochem. J. **42**, 238–250 (1948)
29. Schwimmer, S., Bevenue, A.: Reagent for differentiation of 1,4- and 1,6-linked glucosaccharides. Science **123**, 543–544 (1956). doi:10.1126/science.123.3196.543
30. Banny, T.M., Clark, G.: The new domestic cresyl echt violet. Stain Technol. **25**, 195–196 (1950)
31. Lowry, O.H., Rosebrough, N.J., Farr, A.L., Randall, R.J.: Protein measurement with the folin phenol reagent. J. Biol. Chem. **193**, 265–275 (1951)
32. Gruneberg, H.: Grey-lethal, a new mutation in the house mouse. J. Hered. **27**, 105–109 (1936)
33. Walker, D.G.: Spleen cells transmit osteopetrosis in mice. Science **190**, 785–787 (1975). doi:10.1126/science.1198094
34. Matthieu, J.M., Widmer, S., Herschkowitz, N.: Biochemical changes in mouse brain composition during myelination. Brain Res. **55**, 391–402 (1973). doi:10.1016/0006-8993(73)90304-1
35. Chen, C.S., Patterson, M.C., Wheatley, C.L., O'Brien, J.F., Pagano, R.E.: Broad screening test for sphingolipid-storage diseases. Lancet **354**, 901–905 (1999). doi:10.1016/S0140-6736(98)10034-X
36. Chigorno, V., Tettamanti, G., Sonnino, S.: Metabolic processing of gangliosides by normal and Salla human fibroblasts in culture. A study performed by administering radioactive GM3 ganglioside. J. Biol. Chem. **271**, 21738–21744 (1996). doi:10.1074/jbc.271.36.21738
37. Utsumi, K., Tsuji, A., Kase, R., Tanaka, A., Tanaka, T., Uyama, E., *et al.*: Western blotting analysis of the beta-hexosaminidase alpha- and beta-subunits in cultured fibroblasts from cases of various forms of GM2 gangliosidosis. Acta Neurol. Scand. **105**, 427–430 (2002). doi:10.1034/j.1600-0404.2002.01097.x
38. Gieselmann, V.: Lysosomal storage diseases. Biochim. Biophys. Acta **1270**, 103–136 (1995)
39. Huwiler, A., Kolter, T., Pfeilschifter, J., Sandhoff, K.: Physiology and pathophysiology of sphingolipid metabolism and signaling. Biochim. Biophys. Acta **1485**, 63–99 (2000)
40. Igisu, H., Suzuki, K.: Progressive accumulation of toxic metabolite in a genetic leukodystrophy. Science **224**, 753–755 (1984). doi:10.1126/science.6719111
41. Suzuki, K.: Twenty five years of the "psychosine hypothesis": a personal perspective of its history and present status. Neurochem. Res. **23**, 251–259 (1998). doi:10.1023/A:1022436928925
42. Sonnino, S., Mauri, L., Chigorno, V., Prinetti, A.: Gangliosides as components of lipid membrane domains. Glycobiology **17**, 1R–13R (2007). doi:10.1093/glycob/cwl052
43. Reddy, A., Caler, E.V., Andrews, N.W.: Plasma membrane repair is mediated by Ca(2+)-regulated exocytosis of lysosomes. Cell **106**, 157–169 (2001). doi:10.1016/S0092-8674(01)00421-4
44. Allinquant, B., Hantraye, P., Mailleux, P., Moya, K., Bouillot, C., Prochiantz, A.: Downregulation of amyloid precursor protein inhibits neurite outgrowth in vitro. J. Cell Biol. **128**, 919–927 (1995). doi:10.1083/jcb.128.5.919
45. Ikezu, T., Trapp, B.D., Song, K.S., Schlegel, A., Lisanti, M.P., Okamoto, T.: Caveolae, plasma membrane microdomains for alpha-secretase-mediated processing of the amyloid precursor protein. J. Biol. Chem. **273**, 10485–10495 (1998). doi:10.1074/jbc.273.17.10485
46. Simons, M., Keller, P., De Strooper, B., Beyreuther, K., Dotti, C. G., Simons, K.: Cholesterol depletion inhibits the generation of beta-amyloid in hippocampal neurons. Proc. Natl. Acad. Sci. U. S. A. **95**, 6460–6464 (1998). doi:10.1073/pnas.95.11.6460
47. Choo-Smith, L.P., Surewicz, W.K.: The interaction between Alzheimer amyloid beta(1–40) peptide and ganglioside GM1-containing membranes. FEBS Lett. **402**, 95–98 (1997). doi:10.1016/S0014-5793(96)01504-9
48. Fortin, D.L., Troyer, M.D., Nakamura, K., Kubo, S., Anthony, M. D., Edwards, R.H.: Lipid rafts mediate the synaptic localization of alpha-synuclein. J. Neurosci. **24**, 6715–6723 (2004). doi:10.1523/JNEUROSCI.1594-04.2004
49. Benarroch, E.E.: Lipid rafts, protein scaffolds, and neurologic disease. Neurology **69**, 1635–1639 (2007). doi:10.1212/01.wnl.0000279590.22544.c3
50. Vey, M., Pilkuhn, S., Wille, H., Nixon, R., DeArmond, S.J., Smart, E.J., *et al.*: Subcellular colocalization of the cellular and scrapie prion proteins in caveolae-like membranous domains. Proc. Natl. Acad. Sci. U. S. A. **93**, 14945–14949 (1996). doi:10.1073/pnas.93. 25.14945
51. Rodriguez-Lafrasse, C., Vanier, M.T.: Sphingosylphosphorylcholine in Niemann-Pick disease brain: accumulation in type A but not in type B. Neurochem. Res. **24**, 199–205 (1999). doi:10.1023/A:1022501702403
52. Yu, R.K., Bieberich, E., Xia, T., Zeng, G.: Regulation of ganglioside biosynthesis in the nervous system. J. Lipid Res. **45**, 783–793 (2004). doi:10.1194/jlr.R300020-JLR200
53. Maxzud, M.K., Daniotti, J.L., Maccioni, H.J.: Functional coupling of glycosyl transfer steps for synthesis of gangliosides in Golgi membranes from neural retina cells. J. Biol. Chem. **270**, 20207–20214 (1995). doi:10.1074/jbc.270.34.20207
54. Maccioni, H.J.: Glycosylation of glycolipids in the Golgi complex. J. Neurochem. **103**(Suppl 1), 81–90 (2007). doi:10.1111/j.1471-4159.2007.04717.x